Final Draft
of the original manuscript:

Tchaikovsky, A.; Häusler, H.; Kralik, M.; Zitek, A.; Irrgeher, J.; Prohaska, T.:
Analysis of n(87Sr)/n(86Sr), δ88Sr/86SrSRM987 and elemental pattern to characterise groundwater and recharge of saline ponds in a clastic aquifer in East Austria.
In: Isotopes in Environmental and Health Studies. Vol. 55 (2019) 2, 179 - 198.
First published online by Taylor & Francis: 24.03.2019

DOI: 10.1080/10256016.2019.1577832
https://dx.doi.org/10.1080/10256016.2019.1577832

Analysis of $n(^{87}Sr)/n(^{86}Sr)$, $\delta^{88}Sr/^{86}Sr_{SRM987}$ and elemental pattern to characterise groundwater and recharge of saline ponds in a clastic aquifer in East Austria

Anastassiya Tchaikovsky[a], Hermann Häusler[b], Martin Kralik[b], Andreas Zitek[a], Johanna Irrgeher[c,d] and Thomas Prohaska[a,d]

[a]VIRIS Laboratory, Department of Chemistry, University of Natural Resources and Life Sciences Vienna, Tulln, Austria; [b]Department of Environmental Geosciences, University of Vienna, Vienna, Austria; [c]Department for Marine Bioanalytical Chemistry, Helmholtz Centre for Materials and Coastal Research, Institute for Coastal Research, Geesthacht, Germany; [d]Chair of General and Analytical Chemistry, Montanuniversität Leoben, Leoben, Austria

Abstract

Elemental and isotopic pattern of n(87Sr)/n(86Sr) and δ88Sr/86SrSRM987 were used to characterise groundwater and recharge of saline ponds in a clastic aquifer in East Austria. Therefore, shallow, artesian and thermal groundwaters of the investigated aquifer along with rainfall and rivers were analysed using (MC) ICP-MS. The n(87Sr)/n(86Sr) ratio and elemental pattern changed with aquifer depth as a result of progressing bedrock leaching and dissolution with increasing groundwater residence time. The n(87Sr)/n(86Sr) ratio of shallow groundwater below saline ponds of 0.71019 ± 0.00044 was significantly different from thermal groundwater of 0.71205 ± 0.00035 (U, k = 2). In contrast to previous theories, this result suggested no recharge of saline ponds by upwelling paleo-seawater. Isotope pattern deconvolution revealed that rainfall accounted to about 60% of the n(87Sr)/n(86Sr) ratio of shallow groundwater below saline ponds. The δ88Sr/86SrSRM987 values of groundwater decreased from about 0.25 ‰ in most shallow, to predominantly negative values of about –0.24 ‰ in artesian groundwater. This result indicated leaching and dissolution of weathered minerals. In turn, the δ88Sr/86SrSRM987 of deep thermal groundwater showed positive values of about 0.12 ‰, which suggested removal of 86Sr from solution by carbonate precipitation. These results highlight the potential of δ88Sr/86SrSRM987 signature as an additional geochemical tracer.

1. Introduction

Strontium isotopes are well-established environmental tracers in hydrologic studies [1–4]. Strontium is a natural non-toxic element consisting of four stable isotopes ^{84}Sr, ^{86}Sr, ^{87}Sr and ^{88}Sr. The isotope displaying the highest variability in nature is ^{87}Sr due to the radioactive β^--decay of ^{87}Rb to ^{87}Sr. In general, the ^{87}Sr isotope abundance is expressed as

the isotope amount ratio $n(^{87}Sr)/n(^{86}Sr)$. (This isotope notation – $n(^{j}Sr)/n(^{i}Sr)$ – is recommended by the Commission on Isotopic Abundances and Atomic Weights of the International Union of Pure and Applied Chemistry (IUPAC) and will be used throughout the publication [5,6]. If the ratio is stated as general ratio, $^{j}Sr/^{i}Sr$ is used.) Its relative amount in nature is a function of the Rb/Sr elemental ratio and the age of the geological bedrock with reported $n(^{87}Sr)/n(^{86}Sr)$ isotope amount ratios between 0.70 and 0.78 [7,8]. Chemical weathering releases strontium from bedrocks to surface water allowing to infer on the lithology of drainage basins [9], to quantify silicate vs. carbonate weathering [10] or to determine strontium inputs to the oceans over geologic history [11].

In groundwater the $n(^{87}Sr)/n(^{86}Sr)$ isotopic composition is determined by the dissolution of the most leachable mineral phases of the bedrock [2,9,12,13]. Montgomery et al. [14] observed a general correlation of the $n(^{87}Sr)/n(^{86}Sr)$ isotope ratio of mineral water and aquifer host rock composition. They reported that water from older rock aquifers had a more radiogenic signature than those from younger rock aquifers. Shand et al. [2] used the $n(^{87}Sr)/n(^{86}Sr)$ isotope ratio to determine sources and mixing relationships of groundwater. Woods et al. [15] attributed differences in the $n(^{87}Sr)/n(^{86}Sr)$ isotope ratio of young and old groundwater to different degrees of water–rock interaction. Therefore, the radiogenic strontium isotope ratio represents a geogenic tracer useful in hydrologic studies e.g. for the inference on the lithologic type and age of the aquifer bedrock, groundwater mixing along flow paths and residence time.

In recent years, advances in mass spectrometry facilitated the determination of the variation of the $n(^{88}Sr)/n(^{86}Sr)$ isotope amount ratio, which had previously been considered constant in nature [16,17]. This isotope ratio is conventionally expressed in the δ-notation relative to the certified reference material NIST SRM 987. (In the 'Guidelines and recommended terms for expressing stable-isotope-ratio and gas-ratio measurement results' the IUPAC recommended a notation of the isotope ratio as $\delta^{88}Sr/^{86}Sr_{SRM987}$ [5]. It has been reported as important to indicate the reference standard, which is in this case NIST SRM 987.) The reported variation of the $\delta^{88}Sr/^{86}Sr_{SRM987}$ in nature ranges from about −1.1 to + 1.4 ‰ as a result of mass-dependent isotope fractionation [18]. For example, Böhm et al. [19] demonstrated $^{88}Sr/^{86}Sr$ isotope fractionation during inorganic calcite precipitation. DeSouza et al. [20] found preferential uptake of ^{86}Sr by plants such that their $\delta^{88}Sr/^{86}Sr_{SRM987}$ value was significantly lower than those of soils in which they grew in. Halicz et al. [21] reported strontium isotope fractionation in soils which they attributed to different degrees of chemical weathering. These observations suggested that the $\delta^{88}Sr/^{86}Sr_{SRM987}$ has a high potential for the investigation of eco-geochemical processes as well.

The $^{88}Sr/^{86}Sr$ ratio of groundwater bears therefore a high potential to give additional insights on the genesis of minerals which form the aquifer host rock as well as geochemical reactions such as precipitation.

In this work, the applicability of $n(^{87}Sr)/n(^{86}Sr)$, $\delta^{88}Sr/^{86}Sr_{SRM987}$ and elemental pattern for groundwater characterisation was investigated in the clastic aquifer of the Neogene Lake Neusiedl-Seewinkel Basin, East Austria. It consists of about 1000 m thick brackish to fluvial deposits forming the bedrock of shallow, deeper artesian and deep thermal aquifers. A peculiarity of the study area is the occurrence of larger saline lakes and smaller saline ponds. Tauber [22] postulated that their saline water resulted from upwelling of deep marine connate water of Badenian to Sarmatian age along faults. This hypothesis

was termed 'ascending theory' and was supported by ice-free ponds during winter, which were interpreted as a result of ascending thermal water. However, recent research demonstrated that these ice-free ponds resulted from emanating methane, which prevented ice formation [23,24]. These findings challenged the hypothesis of upwelling thermal groundwater, calling out for further investigations of groundwater of the clastic aquifer.

The two major aims of this work were 1) to evaluate the potential of combining the $n(^{87}Sr)/n(^{86}Sr)$, $\delta^{88}Sr/^{86}Sr_{SRM987}$ and elemental pattern for groundwater characterisation along the vertical profile of the clastic aquifer, and 2) to use the isotopic and elemental information to investigate potential recharge sources to shallow groundwater below saline ponds of the Lake Neusiedl-Seewinkel Basin.

2. Material and methods

2.1. Study area

The Lake Neusiedl-Seewinkel Basin is located 40 km southeast of Vienna in East Austria, Central Europe (Figure 1). It encompasses an area of approximately 1100 km^2 and represents a lowland region characterised by warm climate and low amounts of wet precipitation [25,26]. A large part of the study area is covered by the second largest endorheic lake in Europe, Lake Neusiedl and the Lake District Seewinkel. The surroundings of these open water systems represent an important habitat for migrating birds and are protected by the Ramsar Convention on Wetlands [27,28].

The study area represents a subsided basin filled with marine sediments of Badenian to Sarmatian age (11.5–16 Ma) and brackish to lacustrine sediments of Pannonian age (5.5–11.5 Ma) deposited by the Paratethys, the Neogene remnant of the former Tethys ocean. This resulted in the formation of a 1000 m thick clastic aquifer comprised of a mixture and intercalation of gravel, sand, silt and clay [24]. In the Quaternary (ca. 1.8 Ma), within fluvial deposits a saline soil layer came into existence in the Seewinkel underlying saline lakes and saline ponds [31].

The Leitha Mountains to the north and the Rosalia Mountains and the Rust Range to the west represent the potential recharge area of the clastic aquifer [25]. The altitude of these elevations is 250–700 m above the sea level. The Leitha and Rosalia Mountains consist of crystalline basement predominantly made up of metamorphic Paleozoic and Mesozoic schists, with Triassic dolomites and quartzites as well as Neogene limestone deposits at the flanks ([24]; Figure 1).

The investigated clastic aquifer comprised of three floors: shallow groundwater, artesian groundwater and deep thermal groundwater. The latter displays temperatures of more than 35 °C and is used in spas [32], while some artesian springs are used as potable and mineral water [24]. Studies showed no connection between the groundwater of these three clastic aquifer-types and the Lake Neusiedl [23,33].

2.2. Sample collection

Figure 1 shows the twenty-six investigated sampling sites. Water samples were collected from three rivers draining the Leitha and Rosalia Mountains (ID 1–3) as well as five shallow

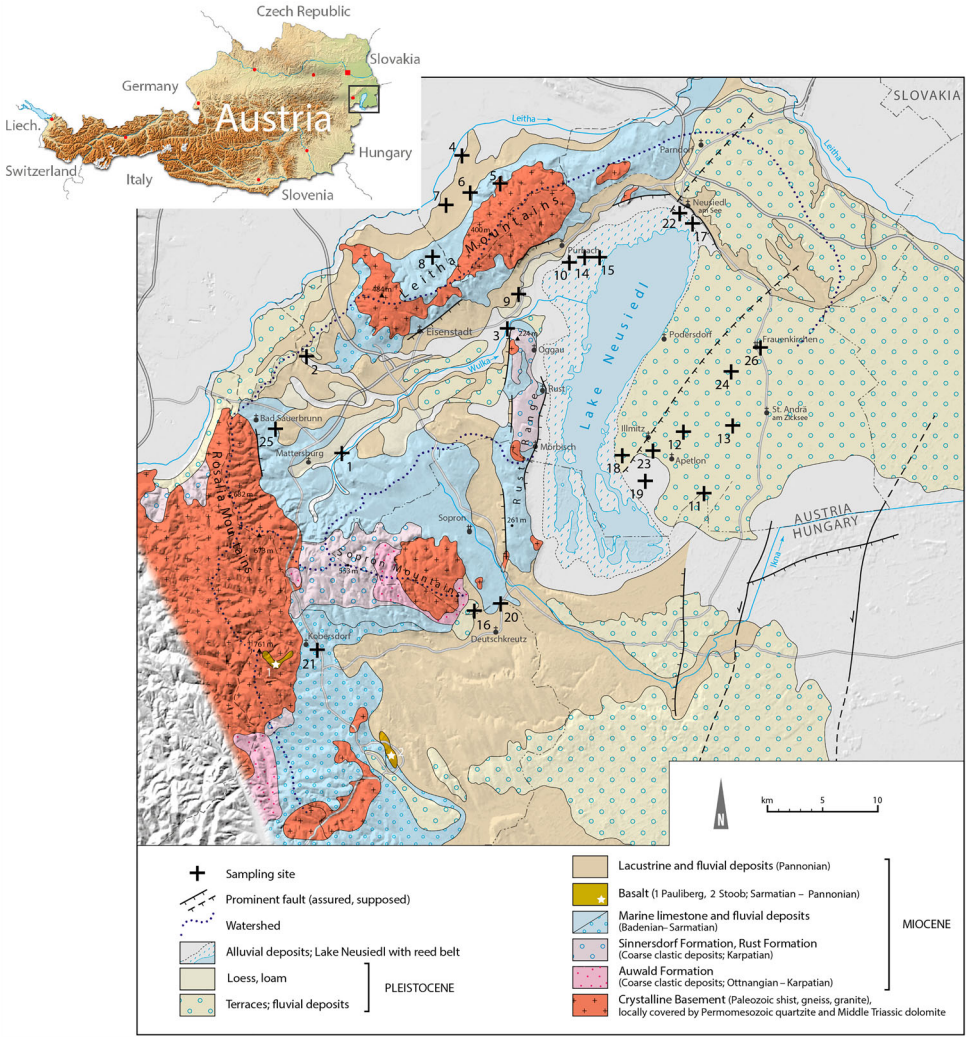

Figure 1. Sampling sites and geological map of the study area, Burgenland, East Austria modified after Herrmann et al. and Brix et al. [29,30].

(ID 11–15), eight artesian (ID 16–23) and two thermal (ID 24, 25) clastic aquifers. All samples were collected in pre-cleaned polyethylene bottles following the procedure by Mook et al. [34]. Surface and spring water was collected below surface. Groundwater was sampled from wells to depths that ranged from 5 to 1050 m below ground surface (bgs). The electrical conductivity (EC) was determined in-field using a portable conductivity meter (Cond 3110, WTW, Weilheim i. OB, Germany). Local wet precipitation was sampled in Frauenkirchen in the Seewinkel (ID 26) in pre-cleaned polyethylene bottles. In addition, the VIRIS laboratory provided the $n(^{87}Sr)/n(^{86}Sr)$ strontium isotope amount ratio data of seven additional surface water samples from the assumed recharge area of the Leitha Mountains (ID 4–10) collected within the course of another project. River water was sampled using pre-cleaned polyethylene bottles and analysed for their strontium

Table 1. Hydrological and chemical parameters of investigated water samples; n.a. denotes not analysed; *LOQ* of K = 2.06 µg g^{-1} and Ca = 6.71 µg g^{-1}; uncertainties of the electrical conductivity (EC), elemental amount fractions, $n(^{87}Sr)/n(^{86}Sr)$ ratios and $\delta^{88}Sr/^{86}Sr_{SRM987}$ values correspond to 0.05%, 10%, 0.00025 and 0.10 ‰ (U, $k = 2$), respectively; significant numbers of digits are given according to EURACHEM guidelines.

ID	Location	Water Source	Lat	Long	Date	Type	Lithology	Depth m bgs	EC µS cm^{-1}	Na µg g^{-1}	Mg µg g^{-1}	K µg g^{-1}	Ca µg g^{-1}	Sr µg g^{-1}	$n(^{87}Sr)/n(^{86}Sr)$	$\delta^{88}Sr/^{86}Sr_{SRM987}$ ‰
1	Wulka catchment	Marz brook	47.738908	16.418761	Jul 2013	Surface	ALLUV	0	812	22.8	32	4.2	109	0.283	0.71048	−0.14
2	Wulka catchment	Zillingtal brook	47.828228	16.389267	Jul 2013	Surface	ALLUV	0	1094	13.2	112	<LOQ	178	0.33	0.71137	0.14
3	Wulka catchment	River Wulka	47.850964	16.630158	Jul 2013	Surface	ALLUV	0	1053	48	47	13.9	111	0.42	0.71019	0.21
4	Leitha Mountains	Ar brook (down hill)	47.980540	16.563880	Jul 2011	Surface	ALLUV	0	n.a.	n.a.	n.a.	n.a.	n.a.	n.a.	0.71064	n.a.
5	Leitha Mountains	Ar brook (up hill)	47.957800	16.586430	Jul 2011	Surface	ALLUV	0	n.a.	n.a.	n.a.	n.a.	n.a.	n.a.	0.71267	n.a.
6	Leitha Mountains	Au brook	47.948810	16.559170	Jul 2011	Surface	ALLUV	0	n.a.	n.a.	n.a.	n.a.	n.a.	n.a.	0.71074	n.a.
7	Leitha Mountains	Hofer-Grenz brook	47.944370	16.541040	Jul 2011	Surface	ALLUV	0	n.a.	n.a.	n.a.	n.a.	n.a.	n.a.	0.70985	n.a.
8	Leitha Mountains	Erl brook	47.918990	16.541710	Jul 2011	Surface	ALLUV	0	n.a.	n.a.	n.a.	n.a.	n.a.	n.a.	0.70907	n.a.
9	Leitha Mountains	Wolfsbrunn brook	47.881060	16.647480	Jul 2011	Surface	ALLUV	0	n.a.	n.a.	n.a.	n.a.	n.a.	n.a.	0.71106	n.a.
10	Leitha Mountains	Anger brook	47.907450	16.705790	Jul 2011	Surface	ALLUV	0	n.a.	n.a.	n.a.	n.a.	n.a.	n.a.	0.70993	n.a.
11	Seewinkel	Borehole Arbesthau Lacke	47.906889	16.699869	Oct 2013	Shallow	SAL	2	2500	320	118	23.8	130	1.62	0.71067	0.28
12	Seewinkel	Borehole Xix-See	47.907181	16.700314	Oct 2013	Shallow	SAL	2	3390	742	110	27.5	249	0.91	0.71003	0.23
13	Seewinkel	Borehole Lange Lacke	47.719472	16.845906	Oct 2013	Shallow	SAL	2	1722	266	229	36	681	1.39	0.70987	−0.05
14	Purbach	Fischergasse	47.759294	16.842006	Oct 2013	Shallow	CLAST	5	947	41	39	16.2	49	0.50	0.71029	0.25
15	Purbach	Purgina	47.759394	16.885000	Oct 2013	Shallow	CLAST	5	8321	1229	588	39	322	3.7	0.70901	0.23
16	Deutschkreutz	Rudolfsquelle	47.945225	16.847833	Aug 2013	Artesian	CLAST	17	2970	409	67	23.1	228	2.07	0.71212	0.25
17	Neusiedl	Klosterschule	47.951683	16.835519	Jul 2013	Artesian	CLAST	56	714	22.7	33	2.09	91	0.187	0.70993	−0.45
18	Seewinkel	Sandeck	47.700036	16.809928	Jul 2013	Artesian	CLAST	68	903	74	45	2.20	74	0.71	0.71086	−0.18
19	Seewinkel	Neudegg	47.733781	16.766411	Jul 2013	Artesian	CLAST	85	530	27.4	34	1.83	52	0.67	0.71094	−0.12
20	Deutschkreutz	Juvina	47.761728	16.799894	Aug 2013	Artesian	CLAST	100	2520	281	58	18.1	249	1.92	0.71183	−0.09
21	Kobersdorf	Gemeindequelle	47.619442	16.619722	Sep 2013	Artesian	CLAST	125	2640	190	69	18.4	340	2.54	0.71378	−0.38
22	Neusiedl	District commisson	47.618917	16.620022	Jul 2013	Artesian	CLAST	138	4290	490	237	41	399	13.8	0.70952	−0.23
23	Illmitz	Bartholomäusquelle	47.595683	16.394278	Jul 2013	Artesian	CLAST	190	4030	958	35	11.5	53	0.75	0.71137	−0.23
24	Frauenkirchen	Spa	47.808778	16.915939	Aug 2013	Thermal	CLAST	865	1426	329	4.2	4.2	<LOQ	0.46	0.71182	0.03
25	Bad Sauerbrunn	Spa	47.780453	16.339136	Aug 2013	Thermal	CLAST	1050	2370	785	62	28.8	59	5.2	0.71228	0.20
26	Frauenkirchen	Bahnstraße	47.839736	16.917775	Sep 2018	Precipitation	–	–	n.a.	0.15	0.28	0.22	3.9	0.0053	0.70887	0.20

isotope ratios following standard protocols [35,36]. Details on the geographical location and sampling time are given in Table 1.

2.3. Elemental and strontium isotopic analysis

Water and wet precipitation samples (ID 1–3 and 11–26) were analysed for their elemental and strontium isotopic composition at the University of Natural Resources and Life Sciences Vienna, Department of Chemistry. Preparatory laboratory work was performed in an ISO class 8 clean room according to ISO 14644-1. Laboratory water type I (18 MΩ cm, F + L GmbH, Vienna, Austria) was further purified using a sub-boiling distillation system (Milestone-MLS GmbH, Leutkirch, Germany). Nitric acid (p.a., 65% *w/w*; Merck-Millipore, Darmstadt, Germany) was double sub-boiled in a DST-1000 sub-boiling distillation system (AHF Analysentechnik, Tübingen, Germany) previous to use in the laboratory. All laboratory consumables (polyethylene bottles, tubes, pipette tips) were double acid washed (10% and 1% HNO_3 *w/w*) before use.

Water samples were acidified to 2% HNO_3 (*v/v*) and filtered using a 0.45 µm pore size filter (Sartorius, Göttingen, Germany). The elemental composition of Na, Mg, K, Ca and Sr in water was measured using an inductively coupled plasma quadrupole mass spectrometer (ICP-QMS, NexION 300 D or Elan DRC-e, PerkinElmer, Waltham, USA) in standard mode using a PFA (perfluoroalkoxy) nebuliser (Microflow ST Nebulizer, Elemental Scientific Inc., Nebraska, USA) in combination with a cyclonic spray chamber (PerkinElmer). Samples were diluted as required for the working range of the calibration. Elemental amount fractions were determined following blank correction, normalisation to indium as internal normalisation standard (single element ICP-MS standard, CertiPur, Merck, Darmstadt, Germany) and external calibration applying a 5–point calibration (multi elemental ICP-MS standard VI, CertiPur, Merck). The limit of quantification (*LOQ*) was calculated as equivalent to ten times the standard deviation of the instrument blank taking into account the dilution factor. Results were validated using in-house quality control standards and certified reference materials SLRS-5 river water (National Research Council Canada, Ottawa, Canada) and IAPSO seawater standard (Batch num. P143, OSIL Ltd, Havant, UK) processed in the same way as the samples. The measured values of these elements in the reference materials and the in-house quality-control standard were in agreement to their certified or target values (Table S1 Supplementary material; [37,38]).

Prior to the strontium isotope ratio measurements water samples underwent Sr/matrix separation using a strontium specific extraction resin (Triskem, Bruz, France) following a protocol of Tchaikovsky et al. [39]. Subsequently, the $n(^{87}Sr)/n(^{86}Sr)$, $n(^{88}Sr)/n(^{86}Sr)$ and $n(^{84}Sr)/n(^{86}Sr)$ ratios of the investigated water samples were assessed using a multi-collector inductively coupled plasma mass spectrometer (MC ICP-MS, Nu Plasma HR, Nu Instruments Ltd., Wrexham, UK) equipped with a self-aspirating PFA nebuliser (Microflow ST Nebulizer, Elemental Scientific Inc.) connected to a desolvation unit (either DSN-100, Nu Instruments or Aridus II, Cetac Technologies, Omaha, Nebraska). Strontium isotope ratios were corrected for blank, residual ^{87}Rb and instrumental isotope fractionation according to the procedure described by Horsky et al. [36].

The instrumental isotope fractionation of the $n(^{87}Sr)/n(^{86}Sr)$, $n(^{88}Sr)/n(^{86}Sr)$ and $n(^{84}Sr)/n(^{86}Sr)$ ratios were corrected by a combination of internal inter-elemental correction using

zirconium as an internal isotope standard (single element ICP-MS standard, Inorganic Ventures, Christiansburg, USA) and standard-sample-bracketing using the isotope certified reference material NIST SRM 987 (National Institute of Standards and Technology, Gaithersburg, USA) [40]. This calibration approach corrects for mass-dependent and mass-independent instrumental isotope mass fractionation [41]. The final ratio corresponds to the absolute isotope ratio, reflecting both the radiogenic contribution and mass-dependent fractionation for $n(^{87}Sr)/n(^{86}Sr)$ and variation of $n(^{88}Sr)/n(^{86}Sr)$ and $n(^{88}Sr)/n(^{84}Sr)$ as a consequence of mass-dependent natural fractionation. The $n(^{88}Sr)/n(^{86}Sr)$ ratio is reported as $\delta^{88}Sr/^{86}Sr_{SRM987}$ value. This value is calculated as relative difference (in ‰) to the certified $n(^{88}Sr)/n(^{86}Sr)$ amount ratio of NIST SRM 987. The repeatability (i.e. measurement precision [42]) of the $n(^{87}Sr)/n(^{86}Sr)$ ratio and the $\delta^{88}Sr/^{86}Sr_{SRM987}$ value accounted to 0.000032 and 0.03 ‰, respectively and was determined using the NIST SRM 987 bracketing standard under the same measurement conditions by the same operator on the same measuring system.

The reference material IAPSO was subjected to the same preparation procedure as the samples. Furthermore, the NIST SRM 987 was separated to monitor potential on-column fractionation. The determined $n(^{87}Sr)/n(^{86}Sr)$ ratios of the NIST SRM 987 and IAPSO accounted to 0.71015 ± 0.00044 ($n = 8$; U, $k = 2$) and 0.70931 ± 0.00029 ($n = 2$; U, $k = 2$), respectively and were in agreement with the reference values of 0.71034 ± 0.00026 (U, $k = 2$) and 0.70931 ± 0.00009 ($n = 10$; 2 *SE*; [43]). The measured $n(^{88}Sr)/n(^{86}Sr)$ ratios of the NIST SRM 987 and the IAPSO corresponded to 8.3793 ± 0.0049 ($n = 8$; U, $k = 2$; reference value 8.3786 ± 0.0033) and 8.3817 ± 0.0039 ($n = 2$; U, $k = 2$; reference value 8.38183 ± 0.00004, $n = 10$; 2 *SE*; [43]), respectively. This corresponds to $\delta^{88}Sr/^{86}Sr_{SRM987}$ values of the NIST SRM 987 of 0.09 ‰ ± 0.48 ‰ ($n = 8$; U, $k = 2$) and the IAPSO of 0.37 ‰ ± 0.22 ‰ ($n = 2$; U, $k = 2$), respectively which overlapped with the target values within limits of uncertainty (Table S1 Supplementary material; uncertainties in this study correspond to the expanded combined uncertainty, see below; sample heterogeneity was the biggest source to the uncertainty of the NIST SRM 987 and IAPSO).

2.4. Measurement uncertainty

The measurement uncertainty indicates the quality of the analytical result and represents the combination of all uncertainty contributions (e.g. measurement precision, blank, heterogeneity of the samples, etc.) to the measurement result [44]. Uncertainties were calculated in a step-by-step procedure following the Kragten approach [45]. If not stated elsewise, all uncertainties in this study correspond to the expanded uncertainty (U, $k = 2$) ($k = 2$ corresponds to a confidence level of 95%).

Following to the procedure by Horsky et al. the uncertainties of the strontium isotope ratios were determined taking into account the uncertainties of the blank, measurement precision, instrumental isotopic fractionation correction, heterogeneity of the samples and ^{87}Rb-correction [36]. The uncertainty of the $n(^{87}Sr)/n(^{86}Sr)$ and the $\delta^{88}Sr/^{86}Sr_{SRM987}$ value accounted to 0.00025 and 0.10 ‰, respectively. Average elemental and strontium isotopic results included additionally the contribution of the heterogeneity of the samples (i.e. their standard deviation) to the uncertainty. The uncertainty of molar fractions obtained by isotope pattern deconvolution was determined according to Tchaikovsky et al. [39]. The uncertainty of the elemental mass fractions of Na, Mg, K, Ca and Sr accounted to 10%

including the uncertainty contribution of the blank, measurement precision and slope of the calibration curve.

2.5. Isotope pattern deconvolution

Isotope pattern deconvolution (IPD) was used to calculate the contribution of strontium from wet precipitation and leached bedrock to the $n(^{87}Sr)/n(^{86}Sr)$ ratio of shallow groundwater below saline ponds. This chemometrical method is used in multiple-spike isotope dilution mass spectrometry (IDMS) [46], but can also be applied for the calculation of the contribution of natural sources to the strontium isotopic composition of environmental samples [39]. Therefore, the $n(^{87}Sr)/n(^{86}Sr)$, $n(^{88}Sr)/n(^{86}Sr)$ and $n(^{84}Sr)/n(^{86}Sr)$ ratios of the individual components and the mixture have to be assessed. The determined isotope ratios can then be converted into isotope abundances and used as input variables in a set of simple linear equations. Equation 1 shows an example of the linear equation system for a sample comprised of two components, written in the matrix nation. It is composed of the isotope abundances of the isotope i of strontium A^i, the respective molar fractions of the sources $x_{source,n}$ and an error vector e. The molar fractions of the sources $x_{source,n}$ can be determined by multiple-linear regression modelling using the isotope abundances of the individual sources and the sample as input variables in the LINEST-function in Microsoft Excel®.

$$\begin{bmatrix} A^{84}_{sample} \\ A^{86}_{sample} \\ A^{87}_{sample} \\ A^{88}_{sample} \end{bmatrix} = \begin{bmatrix} A^{84}_{source_1} & A^{84}_{source_2} \\ A^{86}_{source_1} & A^{86}_{source_2} \\ A^{87}_{source_1} & A^{87}_{source_2} \\ A^{88}_{source_1} & A^{88}_{source_2} \end{bmatrix} \cdot \begin{bmatrix} x_{source_1} \\ x_{source_2} \end{bmatrix} + \begin{bmatrix} e^{84} \\ e^{86} \\ e^{87} \\ e^{88} \end{bmatrix} \quad (1)$$

As strontium has four stable isotopes, it is possible to construct up to four equations with four unknowns. Thus, IPD allows for determining the contribution of up to four individual sources to the $n(^{87}Sr)/n(^{86}Sr)$ amount ratio of a sample. This represents a specific feature of IPD in comparison to classical mixing model calculations, which allow for the determination of the contribution of two sources to the strontium isotopic composition of a sample only [9]. Furthermore, similar to IDMS calculations, IPD does not require the strontium elemental content of the end members for the calculation. This has the advantage that variables used in IPD are independent of geochemical processes such as evaporation, which can increase the strontium content in the solution, but do not affect the strontium isotopic composition of water [47].

An example on the calculation of the contribution of wet precipitation and the most leachable minerals of the clastic bedrock, represented by thermal water, to the $n(^{87}Sr)/n(^{86}Sr)$ ratio of shallow groundwater below saline ponds by isotope pattern deconvolution and mixing model calculations using Microsoft Excel® is given in the Supplementary Material 2. The uncertainties were calculated using the Kragten approach [45].

2.6. Statistical data evaluation

Statistical data evaluation was performed using SPSS© (IBM SPSS Statistics 24, Armonk, USA). A one sided t-test allowed comparison of the $n(^{87}Sr)/n(^{86}Sr)$ ratios of 1) thermal

groundwater to seawater of Badenian to Pannonian age [11], and 2) wet precipitation to shallow, artesian and thermal groundwater of the clastic aquifer, respectively. Furthermore, a two-sided *t*-test for independent samples was used to investigate potential differences of the $n(^{87}Sr)/n(^{86}Sr)$ ratio of 1) thermal groundwater and shallow groundwater below saline ponds, and 2) shallow groundwater below saline ponds and shallow groundwater extracted from wells of the clastic aquifer. In addition, a two-sided *t*-test for independent samples was used to determine potential differences in the elemental content of calcium between artesian and thermal groundwater. The statistical significance level corresponded to $\alpha = 0.05$. Furthermore, according to the EURACHEM guidelines values which overlap within limits of uncertainty have to be considered equal [44].

3. Results and discussion

Table 1 summarises the determined electrical conductivity (EC), $n(^{87}Sr)/n(^{86}Sr)$ ratios, $\delta^{88}Sr/^{86}Sr_{SRM987}$ values and Na, Mg, K, Ca and Sr elemental composition of surface water, shallow, artesian and thermal groundwater of the clastic aquifer and local precipitation. The lithology comprised of alluvial deposits (ALLUV), saline soils mixed with clastic deposits (SAL) and clastic deposits (CLAST).

3.1. Electrical conductivity of rivers and groundwater

The electrical conductivity of the investigated river water and groundwater of the shallow, artesian and thermal aquifers ranged between 530 µS cm^{-1} (ID 19, Neudegg) and 8321 µS cm^{-1} (ID 15, Purgina). The obtained EC of river and groundwater samples in the Lake Neusield-Seewinkel area were comparable to measured values by Boroviczény et al. [33] and Cuculic et al. [48]. The different mineralisation of the investigated groundwater was determined by the occurrence of different water types within close vicinity as well as variation in the discharge rates [49]. For example, the artesian spring District commission in Neusiedl (ID 22) was a carbonated spring water of magnesium-sodium-calcium-hydrogen-type [49]. In contrast, shallow groundwater of well Purgina in Purbach (ID 15), which showed the highest EC values, was a magnesium-sodium-sulfate-chloride-type mineral water with a pH of 7.8 [49,50]. It exhibited a discharge rate of estimated less than 1 mL s^{-1}, which resulted in the enrichment of this groundwater with leached bedrock minerals. Zötl and Goldbrunner [49] interpreted the high chloride content of about 2500 mg L^{-1} of this groundwater (of a sample analysed in 1963) as a result of upwelling paleo-marine porewater from lower groundwater floors. However, low bromide and iodide content of less than 0.8 mg L^{-1} argued against recharge of this groundwater by paleo-seawater. Furthermore, recent analysis of groundwater from well Purgina in Purbach showed a lower chloride content of 125 mg L^{-1} only [50].

3.2. Elemental composition of precipitation, rivers and groundwater

Figure 2 shows the relative composition of Ca, Mg and Na + K of wet precipitation, rivers and groundwater of the Lake Neusiedl-Seewinkel area. Rainfall showed a Ca-HCO_3-type water composition, which indicated dissolution of calcareous dust in rainwater. Surface water had a Ca,Mg-HCO_3-type water composition reflecting carbonates which form

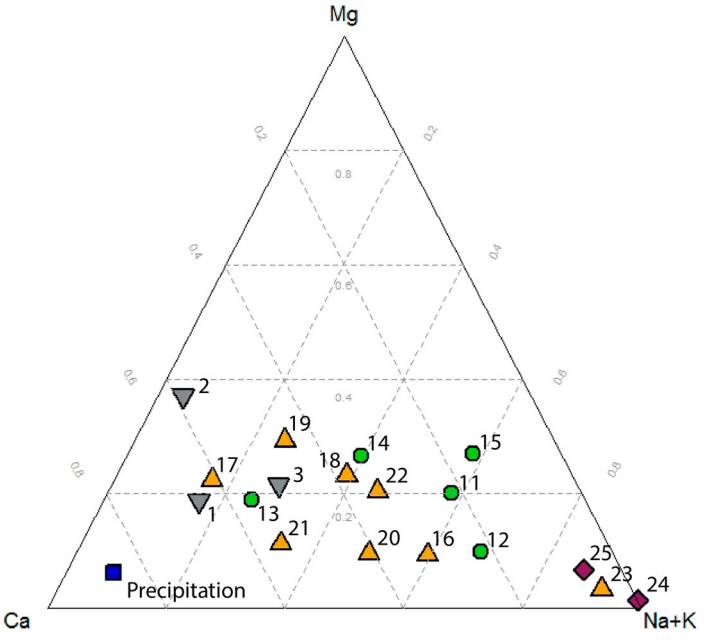

Figure 2. Ternary diagram of major cations in wet precipitation (square), rivers (down-pointing triangles) and groundwater of shallow (circles), artesian (up-pointing triangles) and thermal (diamonds) clastic aquifers.

parts of the drainage basin and dissolve quickly upon contact with water [51]. Groundwater of the clastic aquifer showed a trend from Ca,Mg-HCO_3-type shallow and artesian water towards Na + K-HCO_3-type thermal groundwater. These results were in accordance to findings by Wurm [50].

High sodium and potassium content of thermal groundwater would support the hypothesis of the existence of paleo-seawater in deep aquifers of the Lake Neusiedl-Seewinkel Basin proposed by Tauber [22]. However, the sodium content of 330–780 µg g^{-1} in thermal water of the clastic aquifer was more than one order of magnitude lower than of sea water (Na elemental mass fraction of 10,350 µg g^{-1}; [52]). In addition, the investigated thermal groundwater showed a lower sodium content than known mixtures of meteoric and paleo-seawater of Bad Pirawarth located about 50 km north of the study site (Na elemental mass fraction of 8,000 µg g^{-1}; [32, 49]). Furthermore, Elster et al. [32] and Boroviczény et al. [33] reported $\delta^{18}O$ values of thermal groundwater of the clastic aquifer of the Lake Neusiedl-Seewinkel area ranging between −11.57 and −12.25 ‰, which were in accordance with published $\delta^{18}O$ values of old meteoric water in Central Europe [53]. These values were significantly different to $\delta^{18}O$ of sea water of 0 ‰ [54]. Therefore, the elemental pattern in groundwater of the clastic aquifer rather reflected different degrees of leaching and dissolution of the siliciclastic host rock than mixing of fresh and marine connate water. This hypothesis was further supported by observations in other areas that mineral water extracted from aquifers formed by silicate hard rocks

such as schist, quartzite, granite and sandstone was enriched in Na and K with respect to other cations [51].

3.3. The $n(^{87}Sr)/n(^{86}Sr)$ ratio of groundwater and potential recharge sources

Figure 3 shows the $n(^{87}Sr)/n(^{86}Sr)$ ratios of local precipitation, rivers draining the assumed recharge area of the Leitha and Rosalia mountains, groundwater of the clastic aquifer and a paleo-seawater reference value of Badenian to Pannonian age of 5.5–16 Ma according to Veizer et al. [11]. Precipitation sampled at Frauenkirchen showed a $n(^{87}Sr)/n(^{86}Sr)$ ratio of 0.70889 ± 0.00025 (U, $k = 2$), which was in accordance with strontium isotope values of 0.70875–0.70908 determined in diagenetically modified limestone of the adjacent Leitha Mountains (Figure 1; Personal communication 2017 M. Wagreich, University of Vienna, Department of Geodynamics and Sedimentology). This result fostered the observations that rainwater reflected geochemical signatures of local carbonate dust.

The investigated rivers showed a $n(^{87}Sr)/n(^{86}Sr)$ ratio of 0.71060 ± 0.00099 ($n = 10$; U, $k = 2$) reflecting the lithology of the Leitha and Rosalia Mountains, which are predominantly comprised of metamorphic Paleozoic formations such as schists, gneisses and granites as well as limestone (Figure 1, [24]). The strontium isotopic composition of rivers can serve as a proxy for rainfall infiltrating the ground and forming subsurface runoff

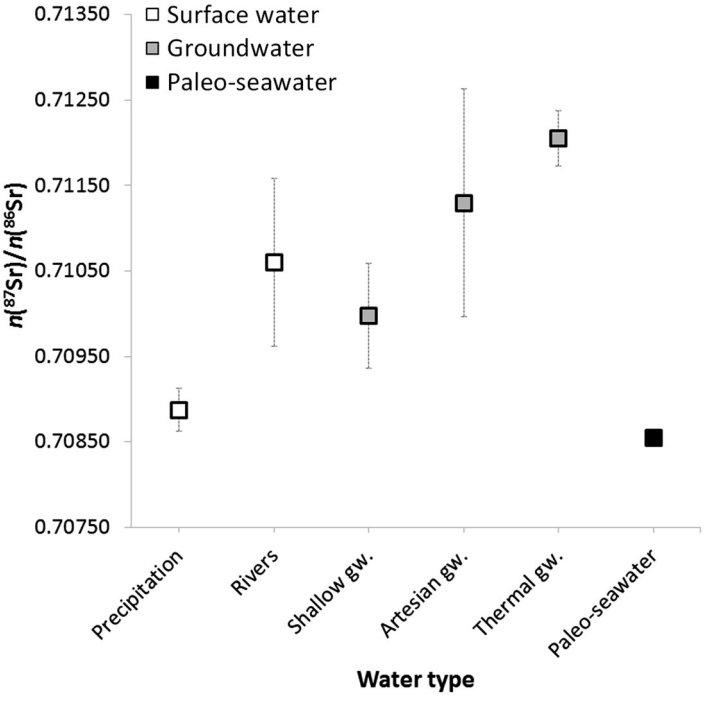

Figure 3. Comparison of the $n(^{87}Sr)/n(^{86}Sr)$ ratios of wet precipitation ($n = 1$), surface water ($n = 10$), shallow ($n = 5$), artesian ($n = 8$) and thermal ($n = 2$) groundwater of the clastic aquifer as well as a paleo-seawater reference value of Badenian to Pannonian age 5.5–16 Ma according to Veizer et al. [11]; error bars correspond to the expanded combined uncertainty (U, $k = 2$).

[1,12,15,55]. Gattinger [25,56] assumed that rivers represented a potential recharge sources to the investigated artesian clastic aquifers.

Shallow groundwater of the clastic aquifer showed an average $n(^{87}Sr)/n(^{86}Sr)$ ratio of 0.70997 ± 0.00063 ($n = 5$; U, $k = 2$). A comparison of the $n(^{87}Sr)/n(^{86}Sr)$ ratio of three shallow groundwater samples obtained below saline ponds (ID 11–13) and two shallow groundwater samples extracted from wells (ID 14 and 15) of the clastic aquifer of the Lake Neusiedl-Seewinkel area revealed no statistical differences (two-sided t-test; $p > 0.05$). The investigated shallow aquifers were not connected to the main first (unconfined) groundwater horizon [24]. Thus, shallow groundwater replenishment from surrounding mountains can be excluded. Boroviczény et al. [33] reported that rainfall represented the main recharge source to shallow aquifers of the Lake Neusiedl-Seewinkel Basin. However, the strontium isotopic composition of groundwater of the clastic aquifer was significantly different from local wet precipitation (one-sample t-test; $p < 0.05$, Figure 3), which indicated strontium inputs from more radiogenic strontium sources.

Very few studies investigated the mineral composition of sediments in the Lake Neusiedl-Seewinkel area. Studies of saline Lake Zicksee in the Seewinkel by Stojanovic et al. [57] showed that silicates determined 37% (*w*/*w*), carbonates 58% (*w*/*w*) and organic matter 5% (*w*/*w*) of the suspended particulate matter. Analysis of turbid lake water at the same site revealed that quartz and plagioclase composed more than half of suspended fine-grained material [48]. These studies investigated the uppermost layer of Seewinkel sediments. Deeper sediments of Pannonian age comprising the bedrock of the clastic aquifer of the Lake Neusiedl-Seewinkel area were not mineralogically investigated yet. They are most likely comprised of mineral and rock particles derived from weathering and erosion of rocks of the adjacent Leitha and Rosalia mountains as well as of the Rust range. These minerals might be predominantly quartz, mica and feldspar, which exhibit higher $n(^{87}Sr)/n(^{86}Sr)$ ratios [2,58] mixed with minerals of Mesozoic carbonates and Neogene Leitha limestone.

Figure 3 shows that the average $n(^{87}Sr)/n(^{86}Sr)$ ratio of groundwater increased from shallow (0.70997 ± 0.00063, $n = 5$; U, $k = 2$) to deeper artesian (0.7113 ± 0.0013; $n = 8$; U, $k = 2$) and deep thermal (0.71205 ± 0.00035; $n = 2$; U, $k = 2$) groundwater. Shallow groundwater has a mean groundwater residence time of several tens of years, while thermal groundwater has a mean groundwater residence time of more than 35,000 years [33]. Thus, the increase of the $n(^{87}Sr)/n(^{86}Sr)$ ratios of groundwater with depth could be associated with increased bedrock leaching and dissolution due to longer water–rock interaction. The large variation of the strontium isotope ratio of artesian water indicated different degrees of aquifer host rock leaching and dissolution, which could be influenced by variation in temperature, CO_2 concentration and residence time [33].

The average strontium isotope ratio of thermal groundwater of 0.71205 ± 0.00035 ($n = 2$; U, $k = 2$) was significantly different from published values of seawater at time of aquifer formation (0.70855; Badenium to Pannonium of 5.5–16 Ma; one-sample t-test; $p < 0.05$; [11]; Figure 3) as well as shallow groundwater below saline ponds (0.71019 ± 0.00044; $n = 3$; U, $k = 2$; two-sided t-test; $p < 0.05$). These results further supported the observation that deep groundwater of the clastic aquifer was not of marine origin. Furthermore, these findings challenged the 'ascending theory' indicating no discharge of upwelling thermal water to shallow groundwater below saline ponds. Consequently, shallow groundwater

most likely derived its strontium isotope pattern from rainfall along with leaching and dissolution of the aquifer bedrock.

3.4. The $n(^{87}Sr)/n(^{86}Sr)$ ratio of groundwater below saline ponds

The $n(^{87}Sr)/n(^{86}Sr)$ ratio of shallow groundwater below saline ponds was assumed to be determined by strontium inputs from wet precipitation and host rock leaching and dissolution. Rainwater was considered to reflect the $n(^{87}Sr)/n(^{86}Sr)$ ratios of locally derived dust from the subaerially exposed soil, sediments and bedrock as well as anthropogenic sources [1]. The rock-derived strontium isotope pattern was assumed to represent the most leachable minerals of the siliciclastic aquifer bedrock. This process included dissolution of the most leachable minerals, ion-exchange, leaching of surface sites and release of fluid inclusions [59]. Such considerations were crucial as Shand et al. [2] pointed out that the reaction kinetics of mineral dissolution varies over orders of magnitude. Therefore, the strontium isotope ratio of solutes will be dominated by the most easily leachable minerals of the bedrock [2,9,12,13]. For example, Kralik et al. [60] demonstrated that the $n(^{87}Sr)/n(^{86}Sr)$ ratio of 0.716 of bulk granite at Wolfsthal, North of Lake Neusiedl, was significantly different from the $n(^{87}Sr)/n(^{86}Sr)$ ratio of 0.709 of pore water of the same rock. Thus, the enclosed pore water did not reflect the strontium isotopic composition of the granitic host rock. Therefore, we considered the strontium isotopic signature of the most leachable minerals as an end-member instead of the $n(^{87}Sr)/n(^{86}Sr)$ ratio of the whole rock (i.e. the sum of all mineral phases). Such $n(^{87}Sr)/n(^{86}Sr)$ pattern is reflected by deep and geochemically mature groundwater. For example, Frape et al. [3] reported that deep saline waters and brines of the Canadian Shield almost totally lost their primary isotopic and chemical composition due to extensive, low-temperature water–rock interaction. This observation was supported by investigations of oilfield brines in the USA, which reflected the $n(^{87}Sr)/n(^{86}Sr)$ ratio of the bedrock instead of seawater at the time of deposition of the host rock [61,62].

Thermal water of the investigated area has a mean groundwater residence time of more than 35,000 years and temperatures of more than 35°C. Long groundwater residence times lead to greater water–rock interaction [2]. Furthermore, increased temperatures enhance solubility of siliceous materials [63], which form the bedrock of the clastic aquifer. This assumption was supported by increasing $n(^{87}Sr)/n(^{86}Sr)$ ratio along the vertical profile of the clastic aquifer and high mineralisation of the investigated thermal groundwater. Moreover, studies by Elster et al. [32] showed that the investigated thermal water had $\delta^{18}O$ and $\delta^{2}H$ values of −11.57 to −12.25 ‰ and −81.0 to −93.8 ‰, which suggested meteoric origin. Rainfall has generally low strontium content [1] and, upon contact with rocks, absorbs the strontium isotopic and elemental composition of the most leachable bedrock minerals ([12] and this study). Therefore, we assumed that the primary chemical signal of ancient rainfall in thermal groundwater of the clastic aquifer can be neglected. Consequently, thermal groundwater could be considered as a proxy for the most leachable mineral phases of the host rock of the clastic aquifer of the Lake Neusiedl-Seewinkel Basin.

Table 2 shows the input variables used for the calculation of the contribution of wet precipitation and the most leachable mineral phases of the clastic bedrock, represented by thermal water, to shallow groundwater below saline ponds. The $n(^{87}Sr)/n(^{86}Sr)$,

Table 2. Average strontium isotope ratios and elemental amount fractions of wet precipitation (ID 26), thermal water (ID 24 and 25) and shallow groundwater obtained from boreholes below saline ponds (ID 11, 12 and 13) used as input variables in isotope pattern deconvolution [39] and mixing model calculations according to Faure and Mensing [9]; uncertainties correspond to the expanded combined uncertainty (U, $k = 2$); significant numbers of digits are given according to EURACHEM guidelines.

Water type	Sr µg g^{-1}	U, $k = 2$	$n(^{87}Sr)/n(^{86}Sr)$	U, $k = 2$	$n(^{88}Sr)/n(^{86}Sr)$	U, $k = 2$	$n(^{84}Sr)/n(^{86}Sr)$	U, $k = 2$
Precipitation	0.0053	0.0005	0.70887	0.00025	8.3803	0.0037	0.05654	0.00008
Thermal groundwater	2.8	3.4	0.71205	0.00070	8.3796	0.0042	0.05614	0.00008
Shallow groundwater	1.31	0.39	0.71019	0.00049	8.3799	0.0040	0.05641	0.00030

$n(^{88}Sr)/n(^{86}Sr)$ and $n(^{84}Sr)/n(^{86}Sr)$ ratios of the individual components and the mixture were converted to the respective strontium isotope abundances of ^{84}Sr, ^{86}Sr, ^{87}Sr and ^{88}Sr and used in Equation 1. Isotope pattern deconvolution revealed that rainfall accounted to 58% ± 7% (U, $k = 2$) and bedrock leaching and dissolution to 42% ± 7% (U, $k = 2$) of the $n(^{87}Sr)/n(^{86}Sr)$ ratio of shallow groundwater below saline ponds. These results were confirmed by classical mixing model calculations showing 53% ± 29% (U, $k = 2$) contribution from wet precipitation and 47% ± 29% (U, $k = 2$) from bedrock leaching and dissolution to the strontium isotope pattern of shallow groundwater below saline ponds. While both calculations yielded comparable results, the uncertainty of the molar fractions obtained by isotope pattern deconvolution was about 4-times lower than that of mixing model calculations. The higher uncertainty of the molar fractions determined by the mixing model approach was a result of the high uncertainty of the average elemental amount fraction of thermal water (Sr elemental mass fraction of 2.8 µg g^{-1} ± 3.4 µg g^{-1}; U, $k = 2$; average of sample ID 24 and ID 25). The uncertainty of this variable contributed to 92% of the total uncertainty of the determined molar fractions. (Note: IPD does not require the elemental amount of strontium in the endmembers, see before.) In contrast, although the $n(^{84}Sr)/n(^{86}Sr)$ ratio is often difficult to measure due to the low isotopic abundance of ^{84}Sr of 0.56% ± 0.02% [64], its uncertainty had little influence on the overall uncertainty of the molar fractions obtained by IPD (see uncertainty calculation in the Supplementary Material 2, worksheet IPD_Kragten_Summary). The $n(^{84}Sr)/n(^{86}Sr)$ ratios showed the lowest variation, thus had no significant impact on the results obtained by multiple linear regression modelling.

Consequently, rainfall represented the major strontium source to the $n(^{87}Sr)/n(^{86}Sr)$ isotopic composition of shallow groundwater below saline ponds of the clastic aquifer, while bedrock leaching was less dominant due to short mean groundwater residence time.

3.5. Fractionation of the $\delta^{88}Sr/^{86}Sr_{SRM987}$ in groundwater with depth

Figure 4 shows a $n(^{87}Sr)/n(^{86}Sr)$ vs. $\delta^{88}Sr/^{86}Sr_{SRM987}$ plot of local precipitation, groundwater of shallow, artesian and thermal aquifers and a reference value of modern seawater according to Scher et al. [65]. The $\delta^{88}Sr/^{86}Sr_{SRM987}$ values of about 0.25 ‰ in most shallow groundwater changed to predominantly negative values of about –0.24 ‰ in artesian groundwater and back to positive values of about 0.12 ‰ in thermal groundwater.

Previous investigations in other regions showed that water reflected the $\delta^{88}Sr/^{86}Sr_{SRM987}$ value of the bedrock material [20,43,66–68]. Indeed, $\delta^{88}Sr/^{86}Sr_{SRM987}$ ratio of shallow groundwater were in accordance to wet precipitation potentially reflecting

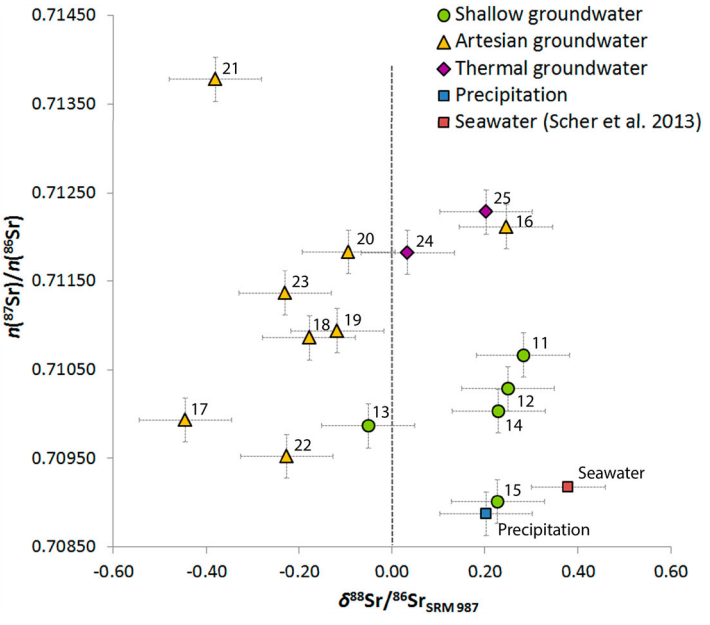

Figure 4. $n(^{87}Sr)/n(^{86}Sr)$ vs. $\delta^{88}Sr/^{86}Sr_{SRM987}$ plot of local wet precipitation (square), shallow (circles), artesian (triangles) and thermal (diamonds) groundwater of the clastic aquifers as well as a seawater reference value (square) according to Scher et al. [65]; line denotes 0 ‰ according to the NIST SRM 987; error bars of this study correspond to the expanded combined uncertainty (U, $k = 2$) and Scher et al. to 2 *SD*.

strontium isotopic composition of local carbonate dust (Figure 4). The shift to negative $\delta^{88}Sr/^{86}Sr_{SRM987}$ values of artesian groundwater indicated leaching and dissolution of aquifer host rock minerals due to longer residence time. Halicz et al. [21] reported $\delta^{88}Sr/^{86}Sr_{SRM987}$ of about –0.17 ‰ in soils which comprised of secondary minerals, mostly clays and quartz grains. Chao et al. [69] observed in laboratory-based leaching experiments that $\delta^{88}Sr/^{86}Sr_{SRM987}$ of residues of Peiliao Shales in Taiwan, composed of quartz, feldspar, illite and chlorite, showed lower $\delta^{88}Sr/^{86}Sr_{SRM987}$ values then the leachates. They attributed these differences to preferential leaching and dissolution of minerals with higher $\delta^{88}Sr/^{86}Sr_{SRM987}$ values. These findings suggested that negative $\delta^{88}Sr/^{86}Sr_{SRM987}$ values of artesian groundwater could potentially reflect leaching and dissolution of bedrock minerals with low $\delta^{88}Sr/^{86}Sr_{SRM987}$, which were formed by weathering processes prior to sedimentation in the aquifer.

The return to positive $\delta^{88}Sr/^{86}Sr_{SRM987}$ values of thermal groundwater in the investigated area could be a result of precipitation of carbonates (and other secondary phases), which preferentially incorporate ^{86}Sr leaving the residual solution enriched in ^{88}Sr [19]. Carbonate precipitation could have been a result of changes in the saturation state of thermal groundwater of the clastic aquifer driven by long water–rock interaction of more than 35,000 years [33], increased temperatures of more than 35°C [32] and pH of about 7–8 [70]. This hypothesis was supported by statistical analysis revealing significantly lower elemental content of calcium in thermal groundwater then in artesian water (two-sided t-test, $p < 0.05$; Figure 5).

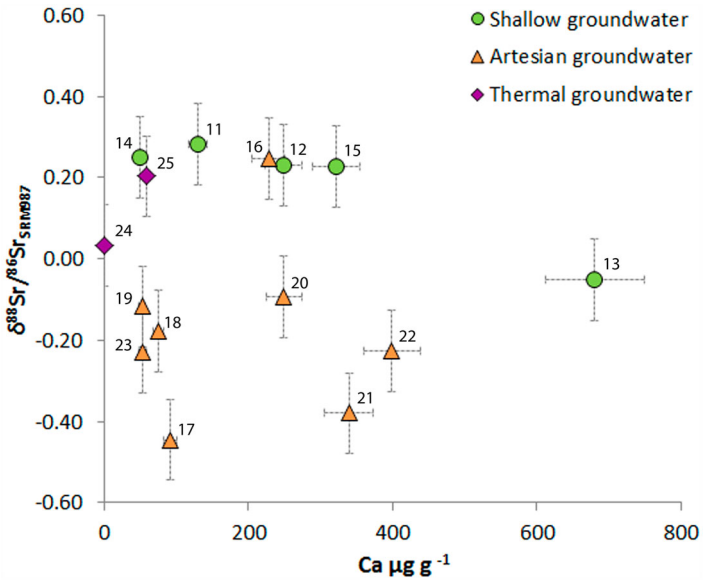

Figure 5. $\delta^{88}Sr/^{86}Sr_{SRM987}$ vs. Ca elemental mass fraction plot of shallow (circles), artesian (triangles) and thermal (diamonds) groundwater of the clastic aquifers; error bars correspond to the expanded combined uncertainty (U, $k = 2$).

Preferential incorporation of the lighter ^{86}Sr isotopes into carbonate precipitates might also be responsible for positive $\delta^{88}Sr/^{86}Sr_{SRM987}$ values of one artesian groundwater sample showing sinter deposits at the well ($\delta^{88}Sr/^{86}Sr_{SRM987}$ of 0.25 ± 0.10 ‰; U, $k = 2$; ID 16; [71]). In contrast, the slightly negative $\delta^{88}Sr/^{86}Sr_{SRM987}$ values of one shallow groundwater below saline lakes of the Seewinkel might indicate higher degrees of aquifer host rock dissolution or influences of other water sources (–0.05 ± 0.10 ‰; U, $k = 2$; ID 13).

4. Conclusion

This study showed that the $n(^{87}Sr)/n(^{86}Sr)$ isotopic and elemental pattern of groundwater of the investigated clastic aquifer changed with depth as a result of progressive aquifer bedrock leaching and dissolution. This process was accompanied by increasing mean groundwater residence time suggesting a continuous groundwater flow path from shallow over artesian to thermal aquifers. The latter showed $n(^{87}Sr)/n(^{86}Sr)$ isotopic and elemental pattern typical for groundwater in host rock aquifers comprised of siliceous minerals, which was in contrast to previous theories suggesting occurrence of marine connate water in deep clastic aquifers of the Lake Neusiedl-Seewinkel region.

The $n(^{87}Sr)/n(^{86}Sr)$ ratio of shallow groundwater below saline ponds was significantly different from thermal groundwater suggesting no upwelling of deep groundwater to the surface. This was further supported by isotope pattern deconvolution revealing that recent rainfall accounted to 58% ± 7% (U, $k = 2$) and bedrock leaching to 42% ± 7% (U, $k = 2$) of the $n(^{87}Sr)/n(^{86}Sr)$ ratio of shallow groundwater below saline ponds.

The $\delta^{88}Sr/^{86}Sr_{SRM987}$ of groundwater changed from positive $\delta^{88}Sr/^{86}Sr_{SRM987}$ values of shallow groundwater to negative values of artesian groundwater, potentially reflecting

leaching and dissolution of bedrock subjected to intense weathering processes before sedimentation. The transition from negative artesian to positive $\delta^{88}Sr/^{86}Sr_{SRM987}$ values of deep thermal groundwater indicated removal of ^{86}Sr from solution, which occurred most likely as a result of carbonate precipitation. These results underline the potential of the $\delta^{88}Sr/^{86}Sr_{SRM987}$ signature as a tracer for the investigation of geochemical processes in aquatic and terrestrial environments.

Further research should focus on the combination of the $n(^{87}Sr)/n(^{86}Sr)$ $\delta^{88}Sr/^{86}Sr_{SRM987}$ and elemental pattern with $\delta^{18}O$ for delineating an enhanced hydrological model of the investigated clastic aquifer. In addition, a series of leaching experiments of cores of the siliciclastic bedrock have the potential to better understand the geochemical processes occurring in the clastic aquifer of the Lake Neusiedl-Seewinkel Basin along with geochemical modelling techniques.

Acknowledgments

The authors would like to acknowledge Christine Opper and Jennifer Sarne for help with sample preparation as well as two anonymous referees for their highly constructive and valuable comments.

Disclosure Statement

No potential conflict of interest was reported by the authors.

References

[1] Capo RC, Stewart BW, Chadwick OA. Strontium isotopes as tracers of ecosystem processes: theory and methods. Geoderma. 1998;82(1–3):197–225.
[2] Shand P, Darbyshire DPF, Love AJ, et al. Sr isotopes in natural waters: applications to source characterisation and water–rock interaction in contrasting landscapes. Appl Geochem. 2009;24(4):574–586.
[3] Frape SK, Fritz P, McNutt RH. Water–rock interaction and chemistry of groundwaters from the Canadian shield. Geochim Cosmochim Acta. 1984;48(8):1617–1627.
[4] Palmer MR, Edmond JM. Controls over the strontium isotope composition of river water. Geochim Cosmochim Acta. 1992;56(5):2099–2111.
[5] Coplen TB. Guidelines and recommended terms for expression of stable-isotope-ratio and gas-ratio measurement results. Rapid Commun Mass Spectrom. 2011;25(17):2538–2560.
[6] Wieser M, Holden N, Coplen T, et al. Atomic weights of the elements 2011 (IUPAC technical report). Pure Appl Chem. 2013;85(5):1047–1078.
[7] Bentley RA. Strontium isotopes from the earth to the archaeological skeleton: a review. J Archaeol Method Theory. 2006;13(3):135–187.
[8] Voerkelius S, Lorenz GD, Rummel S, et al. Strontium isotopic signatures of natural mineral waters, the reference to a simple geological map and its potential for authentication of food. Food Chem. 2010;118(4):933–940.
[9] Faure G, Mensing T. Isotopes: principles and applications. 3rd ed. Hoboken (NJ): John Wiley & Sons; 2005.
[10] Blum J, Erel Y. Radiogenic isotopes in weathering and hydrology. In: Drever JI, editor. Surface and ground water, weathering, and soils. Amsterdam: Elsevier; 2003. p. 365–392.
[11] Veizer J, Ala D, Azmy K, et al. $^{87}Sr/^{86}Sr$, $\delta^{13}C$ and $\delta^{18}O$ evolution of phanerozoic seawater. Chem Geol. 1999;161(1–3):59–88.

[12] Graustein WC. $^{87}Sr/^{86}Sr$ ratios measure the sources and flow of strontium in terrestrial ecosystems. In: Rundel PW, Ehleringer JR, Nagy KA, editor. Stable isotopes in ecological research. New York, NY: Springer; 1989. p. 491–512.
[13] Aberg G. The use of natural strontium isotopes as tracers in environmental studies. Water Air Soil Pollut. 1995;79(1–4):309–322.
[14] Montgomery J, Evans JA, Wildman G. $^{87}Sr/^{86}Sr$ isotope composition of bottled British mineral waters for environmental and forensic purposes. Appl Geochem. 2006;21(10):1626–1634.
[15] Woods T, Fullagar P, Spruill R, et al. Strontium isotopes and major elements as tracers of ground water evolution: example from the upper Castle Hayne aquifer of North Carolina. Groundwater. 2000;38(5):762–771.
[16] Ohno T, Hirata T. Simultaneous determination of mass-dependent isotopic fractionation and radiogenic isotope variation of strontium in geochemical samples by multiple collector-ICP-mass spectrometry. Anal Sci. 2007;23(11):1275–1280.
[17] Fietzke J, Eisenhauer A. Determination of temperature-dependent stable strontium isotope ($^{88}Sr/^{86}Sr$) fractionation via bracketing standard MC-ICP-MS. Geochem Geophys Geosyst. 2006;7(8):Q08009.
[18] Neymark LA, Premo WR, Mel'Nikov NN, et al. Precise determination of $\delta^{88}Sr$ in rocks, minerals, and waters by double-spike TIMS: a powerful tool in the study of geological, hydrological and biological processes. J Anal At Spectrom. 2014;29(1):65–75.
[19] Böhm F, Eisenhauer A, Tang J, et al. Strontium isotope fractionation of planktic foraminifera and inorganic calcite. Geochim Cosmochim Acta. 2012;93:300–314.
[20] Souza GFD, Reynolds BC, Kiczka M, et al. Evidence for mass-dependent isotopic fractionation of strontium in a glaciated granitic watershed. Geochim Cosmochim Acta. 2010;74(9):2596–2614.
[21] Halicz L, Segal I, Fruchter N, et al. Strontium stable isotopes fractionate in the soil environments? Earth Planet Sci Lett. 2008;272(1–2):406–411.
[22] Tauber A. Neusiedlersee – Mineralwasser und Mineralwasserlagerstätte. In: Allgemeine Landestopographie des Burgenlandes. Band 2. Der Verwaltungsbezirk Eisenstadt und die Freistädte Eisenstadt und Rust. Eisenstadt: Amt der Burgenländischen Landesregierung; 1963. p. 786–809. German.
[23] Rank D, Papesch W, Rajner V. Verweilzeiten der jungen Grundwässer im Seewinkel. Illmitz: Biologisches Forschungsinstitut für Burgenland; 1986; German.
[24] Häusler H. Geologische Karte der Republik Österreich 1:50.000, Erläuterungen zur Geologischen Karte 78 Rust. Vienna: Geological Survey of Austria; 2010.
[25] Gattinger T. Das hydrogeologische Einzugsgebiet des Neusiedlersees. Vienna: Geological Survey of Austria; 1975; German.
[26] Auer I, Böhm R, Jurkovic A, et al. HISTALP—historical instrumental climatological surface time series of the greater Alpine region. Int J Climatol. 2007;27(1):17–46.
[27] Winkler H, Berthold P, Leisler B. Monitoring of bird population in the Lake Neusiedl area; [cited 2018 Jul 21]. Available from: http://www.zobodat.at/pdf/STAPFIA_0031_0029-0036.pdf.
[28] Ramsar Convention. [cited 2018 Jul 21]. Available from: https://www.ramsar.org/wetland/austria.
[29] Herrmann P, Pascher G, Pistotnik J. Geologische Karte der Republik Österreich 1:50.000, 78 Rust. Vienna: Geological Survey of Austria; 1993; German.
[30] Brix F, Pascher G. Geologische Karte der Republik Österreich 1:50.000, 77 Eisenstadt. Vienna: Geologic Survey of Austria; 1994; German.
[31] Nestroy O. Den Boden verstehen. Graz: Leopold Stocker Verlag; 2015; German.
[32] Elster D, Goldbrunner J, Wessely G, et al. Erläuterungen zur geologischen Themenkarte Thermalwässer in Österreich 1:500 000. Vienna: Geological Survey of Austria; 2016; p. 296. German.
[33] Boroviczény F, Deák J, Liebe P, et al. Wasserhaushaltsstudie für den Neusiedlersee mit Hilfe der Geophysik und Geochemie 1980–1990.: Institute of Hydraulic Engineering and Water Resources Management, Vienna University of Technology; 1992. German.
[34] Mook WG, Rozanski K, Stichler W, et al. Environmental isotopes in the hydrological cycle – principles and applications. Vol. 1. Paris/Vienna: IAEA-UNESCO; 2000.

[35] Swoboda S, Brunner M, Boulyga SF, et al. Identification of marchfeld asparagus using Sr isotope ratio measurements by MC-ICP-MS. Anal Bioanal Chem. 2008;390(2):487–494.
[36] Horsky M, Irrgeher J, Prohaska T. Evaluation strategies and uncertainty calculation of isotope amount ratios measured by MC ICP-MS on the example of Sr. Anal Bioanal Chem. 2016;408 (2):351–367.
[37] Burton J. The ocean: a global geochemical system. In: Summerhayes C, Thorpe S, editor. Oceanography: An illustrated guide. London: Manson; 1996. p. 165–181.
[38] Yeghicheyan D, Bossy C, Bouhnik Le Coz M, et al. A compilation of silicon, rare earth element and twenty-one other trace element concentrations in the natural river water reference material SLRS-5 (NRC-CNRC). Geostand Geoanal Res. 2013;37(4):449–467.
[39] Tchaikovsky A, Irrgeher J, Zitek A, et al. Isotope pattern deconvolution of different sources of stable strontium isotopes in natural systems. J Anal At Spectrom. 2017;32:2300–2307.
[40] Irrgeher J, Vogel J, Santner J, et al. In: Prohaska T, Irrgeher J, Zitek A, et al., editor. Sector field mass spectrometry for elemental and isotopic analysis. Cambridge: Royal Society of Chemistry; 2015. p. 126–149.
[41] Irrgeher J, Prohaska T, Sturgeon RE, et al. Determination of strontium isotope amount ratios in biological tissues using MC-ICPMS. Anal Methods. 2013;5(7):1687–1694.
[42] ISO. Evaluation of measurement data – Guide to the expression of uncertainty in measurement. Joint Commitee for Guides in Metrology. Standard No.: JCGM. 2008;100:1–134.
[43] Krabbenhöft A, Fietzke J, Eisenhauer A, et al. Determination of radiogenic and stable strontium isotope ratios ($^{87}Sr/^{86}Sr$; $\delta^{88}/^{86}Sr$) by thermal ionization mass spectrometry applying an $^{87}Sr/^{84}Sr$ double spike. J Anal At Spectrom. 2009;24(9):1267–1271.
[44] Ellison SLR, Williams A, editors. EURACHEM/CITAC guide: quantifying uncertainty in analytical measurement; 2012. Available from www.eurachem.org.
[45] Kragten J. Tutorial review. Calculating standard deviations and confidence intervals with a universally applicable spreadsheet technique. Analyst. 1994;119(10):2161–2165.
[46] Garcia Alonso JI, Rodriguez-Gonzalez P. Isotope dilution mass spectrometry. Cambridge: Royal Society of Chemistry; 2013.
[47] Faure G. Principles of isotope geology. 2nd ed. Hoboken (NJ): John Wiley & Sons; 1986.
[48] Cuculić V, Frančišković-Bilinski S, Bilinski H, et al. Multi-methodological approach to evaluate trace elements and major components in wetland system with subsaline and freshwater characteristics. Environ Earth Sci. 2016;75(20):1351.
[49] Zötl J, Goldbrunner J. Die Mineral- und Heilwässer Österreichs: geologische Grundlagen und Spurenelemente. Vienna: Springer; 1993; German.
[50] Wurm M. Hydrogeochemische Methodik zur Klärung von Interationsprozessen von Formations-, Mineral-, Tiefengrund- und öberflächennahen Grundwässern im Einzugsgebiet des Neusiedlersees. Leoben: Montanuniversität Leoben; 2000; German.
[51] Appelo CAJ, Postma D. Minerals and water. geochemistry, groundwater and pollution. 2nd ed. Leiden: A.A. Balkema Publishers; 2010.
[52] Besson P, Degboe J, Berge B, et al. Calcium, Na, K and Mg concentrations in seawater by inductively coupled plasma-atomic emission spectrometry: applications to IAPSO seawater reference material, hydrothermal fluids and synthetic seawater solutions. Geostand Geoanal Res. 2013; 38 (3):355–362.
[53] Rozanski K. Deuterium and oxygen-18 in European groundwaters — Links to atmospheric circulation in the past. Chem Geol Isot Geosci Sect. 1985;52(3):349–363.
[54] Harzhauser M, Latal C, Piller WE. The stable isotope archive of Lake Pannon as a mirror of Late Miocene climate change. Palaeogeogr Palaeoclimatol Palaeoecol. 2007;249(3):335–350.
[55] Jones LM, Faure G. A study of strontium isotopes in lakes and surficial deposits of the ice-free valleys, southern Victoria Land, Antarctica. Chem Geol. 1978;22:107–120.
[56] Gattinger T. The hydrology of Neusiedlersee and its catchment area. Neusiedlersee: the limnology of a shallow lake in Central Europe. The Hague: Dr. W. Junk bv Publishers; 1979.
[57] Stojanovic A, Kogelnig D, Mitteregger B, et al. Major and trace element geochemistry of superficial sediments and suspended particulate matter of shallow saline lakes in Eastern Austria. Chem Erde–Geochem. 2009;69(3):223–234.

[58] Faure G, Powell JL. Strontium isotope geology. Berlin: Springer Verlag; 1972.
[59] McNutt R. – In: Saline water and gases in crystalline rocks. Vol. 33. St. John's, Nfld., Canada: Geological Association of Canada; 1987. p. 81–88. (Geological Association of Canada – Special Paper; 33).
[60] Kralik M, Maringer F, Papesch W, et al., editors. Long-term water percolation around waste disposal sites revealed using natural isotope tracers (^{3}H, ^{18}O, ^{87}Sr, ^{226}Ra/^{238}U). In: Tracers and modelling in hydrogeology. TraM'2000 2000. Liege (Belgium): IAHS. p. 371–375. (IAHS Publ.; 262).
[61] Chaudhuri S. Strontium isotopic composition of several oilfield brines from Kansas and Colorado. Geochim Cosmochim Acta. 1978;42(3):329–331.
[62] Sunwall MT, Pushkar P. The isotopic composition of strontium in brines from petroleum fields of southeastern Ohio. Chem Geol. 1979;24(3):189–197.
[63] Langmuir D. Aqueous environmental geochemistry. Upper Saddle River, NJ: Prentice-Hall, Inc.; 1997.
[64] Meija J, Coplen TB, Berglund M, et al. Isotopic compositions of the elements 2013 (IUPAC technical report). Pure Appl. Chem. 2016;88(3):293–306.
[65] Scher HD, Griffith EM, Buckley WP. Accuracy and precision of ^{88}Sr/^{86}Sr and ^{87}Sr/^{86}Sr measurements by MC-ICPMS compromised by high barium concentrations. Geochem Geophys Geosyst. 2014;15(2):499–508.
[66] Pearce CR, Parkinson IJ, Gaillardet J, et al. Reassessing the stable ($\delta^{88}/^{86}$Sr) and radiogenic (^{87}Sr/^{86}Sr) strontium isotopic composition of marine inputs. Geochim Cosmochim Acta. 2015;157:125–146.
[67] Wei G, Ma J, Liu Y, et al. Seasonal changes in the radiogenic and stable strontium isotopic composition of Xijiang river water: implications for chemical weathering. Chem Geol. 2013;343:67–75.
[68] Krabbenhöft A, Eisenhauer A, Böhm F, et al. Constraining the marine strontium budget with natural strontium isotope fractionations (^{87}Sr/^{86}Sr*, $\delta^{88}/^{86}$Sr) of carbonates, hydrothermal solutions and river waters. Geochim Cosmochim Acta. 2010;74(14):4097–4109.
[69] Chao HC, You CF, Liu HC, et al. Evidence for stable Sr isotope fractionation by silicate weathering in a small sedimentary watershed in southwestern Taiwan. Geochim Cosmochim Acta. 2015;165:324–341.
[70] Webpage. St. Martins Spa Lodge; [cited 2018 Sep 19]. Available from: https://www.stmartins.at/en/water-pools.html.
[71] Kümel F. Geologische Karte der Republik Österreich 1:50.000 Mattersburg – Deutschkreutz. Vienna: Geologic Survey of Austria; 1957; German.